Applied Clay Science 157 (2018) 212–217

Contents lists available at ScienceDirect

Applied Clay Science

journal homepage: www.elsevier.com/locate/clay

Research paper

Preparation of nanocomposites for the removal of phenolic compounds from aqueous solutions

Karina Abigail Hernández-Hernández[a], Javier Illescas[a,*,1], María del Carmen Díaz-Nava[a], Sonia Martínez-Gallegos[a], Claudia Muro-Urista[a], Rosa Elena Ortega-Aguilar[a], Efraín Rodríguez-Alba[b], Ernesto Rivera[b]

[a] Instituto Tecnológico de Toluca, Av. Tecnológico S/N, Col. Agrícola Bellavista, C.P. 52149 Metepec, Estado de México, México
[b] Instituto de Investigaciones en Materiales, Universidad Nacional Autónoma de México, Circuito Exterior S/N, Ciudad Universitaria, C.P. 04510 México D.F, México

ARTICLE INFO

Keywords:
Montmorillonite
Alginate
Nanocomposite
Adsorption
X-ray diffraction data

ABSTRACT

Alginate beads, with and without different types of organo-modified clays, were obtained using a calcium chloride ($CaCl_2$) solution. Firstly, raw clays were organo-modified with a cationic surfactant, hexadecyl trimethylammonium (HDTMA). Then, their cationic exchange capacities (CEC) were calculated and they also were characterized by means of X-ray diffraction (XRD), scanning electron microscopy (SEM), Fourier transform infared (FTIR) spectroscopy, thermogravimetric analysis (TGA) and differential scanning calorimetry (DSC). Afterwards, the obtained polymers and clay polymer nanocomposites (CPN) were carefully characterized by means of the same techniques. Later, different phenol and 4-chlorophenol (4CF) aqueous solutions were prepared and put in contact, for different periods of time, with the synthesized CPN. Phenol and 4CF concentrations were measured by means of UV–vis spectroscopy. Results indicated a successful modification of the raw clay with this cationic surfactant and its incorporation into the alginate polymer matrix. Finally, the maximum removal capacities for both phenolic compounds, 4CF and phenol, were found at qe = 0.334 $mg \cdot g^{-1}$ and qe = 0.118 $mg \cdot g^{-1}$, respectively.

1. Introduction

Nowadays, new challenges are being faced for the development of adsorbent materials that are able to cover the expectations of sustainability and maximum efficiency in the processes of water treatment. One type of material has been studied: composites, which consist of the combination of two or more chemically distinct and insoluble phases that are joined, and their properties and structural performance are superior to those of their constituents acting individually. One of the most studied composite systems is the clay polymer nanocomposite (CPN) (Sinha Ray, 2013). These are classified according to the interactions between the polymer matrix and the silicate layers filler (Sinha Ray, 2013; Gacitua et al., 2005; Pavlidou and Papaspyrides, 2008; Bergaya et al., 2011; Anadão, 2012; Bergaya and Lagaly, 2013; Bergaya et al., 2013): a) intercalated nanocomposites; they are formed when one or more polymer chains, with a well-ordered distribution, are intercalated in an interlayered space of a clay. The stacking of the layers is preserved, with the order along the *c*-axis; the result is a multilayered structure of alternating polymer chains and clay layers with some distance between them; b) exfoliated nanocomposites; these materials are obtained by the total separation of the individual layers of the clay, in a disordered-fashion dispersion of the individual clay layers, in the polymer matrix; finally, c) microcomposites, which are dispersions of fine, micro-sized clay mineral particles in the polymer matrix. Fig. 1 shows the different types of CPN.

The traditional processes to prepare nanocomposites using layered compounds such as reinforcement, especially clays, can be summarized as follows (Biswas and Sinha Ray, 2001; Sinha Ray and Okamoto, 2003; Gacitua et al., 2005; Anadão, 2012): a) exfoliation-adsorption, also called dispersion in solution, the silicate is exfoliated in individual layers in a solvent in which the polymer or prepolymer is soluble (water, toluene, *etc.*); b) *in situ* polymerization, a monomer solution is used as medium for the clay dispersion, and under specific conditions, the polymerization is induced in the interlayer space; and finally, c) melting intercalation, in this method, the silicate is mixed with a thermoplastic polymer matrix in the molten state. Under these conditions, the polymer is carried through the interlayer spaces forming a nanocomposite. Fig. 2 illustrates these methods of nanocomposites synthesis.

* Corresponding author.
E-mail address: fillescasm@toluca.tecnm.mx (J. Illescas).
[1] CONACYT Research Fellow.

https://doi.org/10.1016/j.clay.2018.01.020
Received 12 September 2017; Received in revised form 17 January 2018; Accepted 18 January 2018
Available online 16 February 2018
0169-1317/

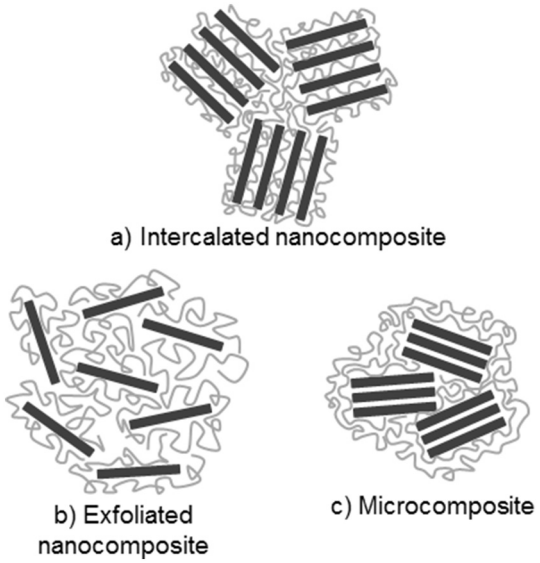

Fig. 1. Structures of the different synthesized clay polymer nanocomposites (CPN).

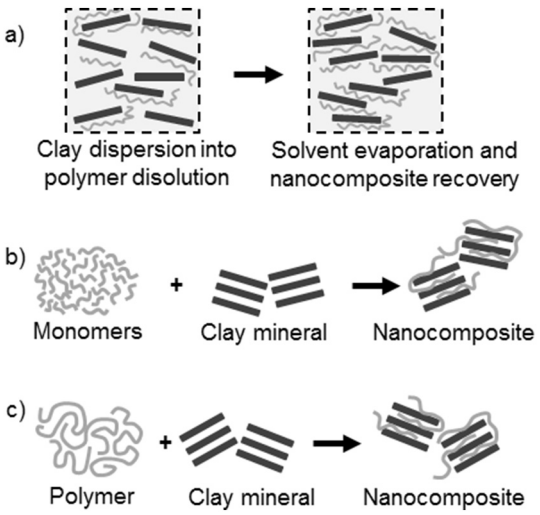

Fig. 2. Different processes for the preparation of CPN.

On the other side, sodium alginate has been recently used in environmental applications, most important for the removal of organic compounds from wastewaters (Feng et al., 2017; Munagapati and Kim, 2017; Pandey et al., 2017; Zhiyu et al., 2017). This polymer shows a sol-gel transition, when its cations are exchanged; namely, when a divalent cation such as calcium is exchanged for two monovalent cations, like sodium. One of the most notable features of alginate is its biocompatibility, as well as its preparation. Moreover, alginate beads are well known for their applications in composites science, as an encapsulant in biomedicine or as a support of different clay materials, like montmorillonite (Mt).

Mt. has been used as a support of alginate beads, because of the improvement on the mechanical properties of the polymer matrix, and because of the simplicity on its organo-modification procedure for the removal of pesticides or polychlorinated biphenyl compounds (PCB) (Silva et al., 2008; Cavallaro et al., 2013; Barreca et al., 2014).

In the present work, the properties of clay alginate nanocomposites were evaluated for the removal of two different compounds, phenol and 4-chlorophenol (4CF), from aqueous solutions. For this purpose, three different types of Mt. were used for the synthesized composites. The first one, an Mt. raw mineral from Puebla State (a mexican province); the second one, an organo-modified Mt. with hexadecyl trimethylammonium ions (HDTMA); and the third one, a commercial clay modified with dialkyl dimethylamine ions (C_{14}-C_{18}). Their morphology and their thermal and spectroscopic characteristics were evaluated, their maximum adsorption capacities were calculated, and their kinetics adsorption models were studied.

2. Experimental

2.1. Materials

All the chemicals and materials used in the synthesis and characterization of clay alginate nanocomposites, as well as those for the phenolic compounds adsorption tests were used as received without any further purification, unless otherwise stated. Sodium alginate, (SA), anhydrous sodium acetate (SAc, $CH_3COO^-Na^+$, FW = 82.03 g/mol, T_b = 337 °C) and phenol (C_6H_6O, FW = 94.11 g/mol, T_b = 182 °C, T_m = 43 °C) were obtained from Meyer. Hexadecyl trimethylammonium bromide (HDTMA-Br, FW = 364.45 g/mol, T_m = 212 °C), a synthetic Mt. organo-modified with dialkyl dimethylamine (C_{14}-C_{18}, FW = 180.1 g/mol, apparent density = 600–1100 kg/m^3, particle size < 20 μm), identified as B3 nanoclay, and 4-chlorophenol (4CF, C_6H_5ClO, FW = 128.56 g/mol, T_b = 220 °C), were obtained from Sigma-Aldrich. Calcium chloride ($CaCl_2$, FW = 110.98 g/mol, T_m = 772 °C) and potassium chloride (KCl, FW = 74.55 g/mol, T_m = 776 °C) were obtained from JT Baker. Finally, two commercial Mt. raw minerals from Puebla State identified by the supplier as B1 and B2 were used.

2.2. Natural clay organo-modifications and cationic exchange capacities (CEC)

The organo-modification of the Mt. raw minerals and their cationic exchange capacities (CEC) were calculated according to the modified Ming and Dixon method (Díaz-Nava et al., 2012). Namely, 25 g of the Mt. raw mineral (B1 or B2) were weighed and placed into a flat bottom ball flask; then, 250 mL of an HDTMA solution (25 eq·L^{-1} or 50 eq·L^{-1}) were added, and magnetically stirred for 15 min. Afterwards, the flask was placed in a shaker bath at 30 °C and 100 rpm for 48 h. Next, the supernatant was removed by decantation and the Mt. was washed with deionized water at 30 °C; a bromide test was performed for each wash until the test resulted negative (6 washes of 200 mL). Subsequently, the Mt. was dried at 70 °C for 24 h, was milled and was passed through a 400 mesh screen to obtain a particle size of 37 μm. Finally, materials were labeled as B1–250 and B2–250 (materials modified with 250 eq·g^{-1}) or B1–500 and B2–500 (materials modified with 500 eq·g^{-1}).

2.3. Clay alginate nanocomposites synthesis

CPN were synthesized according to the next procedure: a solution "A" consisting of 1 g of SA was dissolved in 50 mL of deionized water at 60 °C for 2 h, with magnetic stirring. On the other hand, a solution "B" which consists of 5 g of B1–250, B1–500, B2–250, B2–500 or B3 Mt. were dispersed in 50 mL of deionized water using an ultrasound bath at 30 °C for 2 h. Afterwards, clay dispersions were poured into the SA solution, and magnetic stirred at 30 °C for other 2 h. Then, mixtures were dripped into 500 mL of a 0.1 M $CaCl_2$ solution by means of a peristaltic pump and a micropipette tip. Finally, the obtained beads were agitated for 2 h and refrigerated for 24 h.

2.4. Characterization

2.4.1. Natural and/or organo-modified clays and CPN

X-ray diffraction (XRD) analyses were performed on a Rigaku X-ray diffractometer; model Ultima IV, with the powder method. Samples were run from 1° to 70° in 2θ, with a step size of 0.020° and with a speed of 1.5°/min.

Table 1
CEC of the natural clays obtained by the modified Ming and Dixon method (Díaz-Nava et al., 2012).

Material	CEC ($eq{\cdot}g^{-1}$)
B1	1861.1
B2	1936.4

The morphological characterization of the different types of clay minerals and CPN was performed using a scanning electron microscope SEM JEOL electronic microscope model JSM-6610LV.

FTIR spectra were recorded on an infrared absorption spectrometer with Fourier transform (FTIR Varian 640-IR) equipped with a diamond ATR (attenuated total reflectance) device. The absorption was measured in a wavenumber range between 4000 and 600 cm^{-1} with a resolution of 16 cm^{-1}. To enhance the signal to noise ratio, each spectrum was acquired with 32 scans.

Finally, for the thermal analysis, samples were analyzed in a thermogravimetric analyzer, TA Instruments, model Q 5000 TGA under N_2 atmosphere from 25 to 700 °C at a heating rate of 10 °C·min^{-1}. DSC measurements were conducted in a differential scanning calorimeter TA Instruments, model 2910. For each sample, two consecutive scans were carried out from −80 to 250 °C with a heating rate of 5 °C·min^{-1}, under N_2 atmosphere.

2.4.2. Adsorption of the phenolic compounds

Mixtures of 100 mg of raw or organo-modified Mt., or CPN, and 10 mL of phenol or 4CF solutions (10 $mg{\cdot}L^{-1}$) were shaken for different times, from 0.25 to 72 h, at 25 °C and 100 rpm. Then, samples were decanted and the supernatant was centrifuged in 2 cycles of 4 min at 4000 rpm. Subsequently, phenol and 4CF were analyzed by UV–vis spectroscopy, by means of a Perkin-Elmer Lambda 35 instrument, at different wavelength values: phenol at 270 nm and 4CF at 280 nm. Each experiment was performed in duplicate.

The qe values (equilibrium adsorption capacity) are determined from the adsorption kinetics curve: once the qt values do not change, we can assume that the equilibrium has been reached; therefore, qe = qt.

qt is determined from the next formula:

$$qt = \frac{(Ci - Ct)}{w} * V \quad (1)$$

where Ci is the initial concentration of the phenol solution in $mg{\cdot}L^{-1}$, Ct is the phenol concentration in a determined time t ($mg{\cdot}L^{-1}$), w is the mass of the dry adsorbent material (g) and V is the volume of the solution (L).

3. Results and discussion

3.1. Organo-modification of natural clays

3.1.1. CEC

Table 1 summarizes the CEC results of the natural clays obtained by the modified Ming and Dixon method (Díaz-Nava et al., 2012). These set of results had a similar value and although B2 material had a relatively higher CEC value than B1 material, the adsorption probes confirmed that B1 removed phenol and 4CF more efficiently than B2. Therefore, the presented results consisted of the alginate beads nanocomposites with and without the organo-modified B1 and B1–500 clay minerals and with the synthetic B3 nanoclay.

3.1.2. XRD analysis

Fig. 3 illustrates the obtained XRD patterns from the B1 clay and the B1–500 clay used in this work. It is important to highlight that B1–250 was not employed, since its organo-modification with 250 $eq{\cdot}g^{-1}$ of HDTMA, was not enough to substantially increase its organic affinity, and therefore, its organic-compounds removal properties.

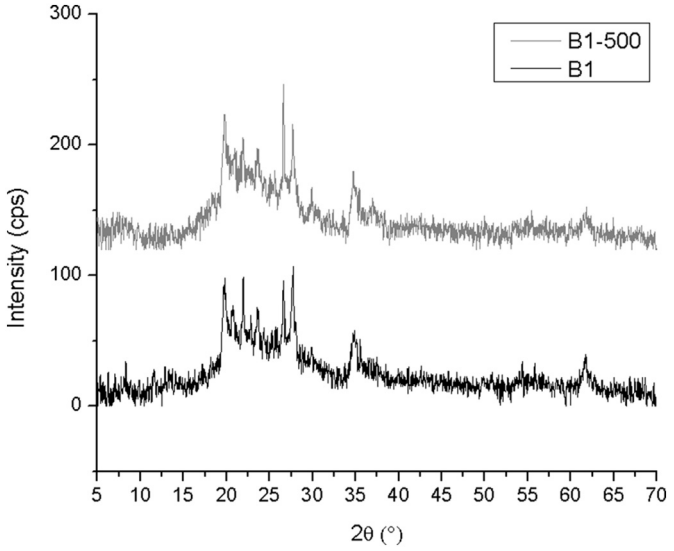

Fig. 3. XRD patterns of the natural clay mineral (B1) and the HDTMA organo-modified clay (B1–500).

According to the XRD patterns, the main clay minerals identified in the samples were: Mt. (JCPDS 00-012-0232), palygorskite (Pal) (JCPDS 00-005-0099), albite (Alb) (JCPDS 00-001-0739) and quartz (JCPDS 00-005-0490). The analyzed clay mineral did not have significant differences after its conditioning with HDTMA. It was confirmed some slight changes in the intensities of some reflections, more probably due to a partial destruction of the laminar structure of the organo-modified clay, owed to its milling process. Therefore, HDTMA surfactant not only was intercalated in the interlayer space of the clay mineral, but also was found on the surface of the modified material.

3.2. CPN characterization

3.2.1. SEM analysis

Fig. 4a and b present micrographs of natural B1 and modified B1–500 clays According to Fig. 4b, the surface of the modified clay mineral had some agglomerates of small particles, which were not identified on the surface of the B1 Mt. raw mineral, Fig. 4a. This change could be associated to the presence of the surfactant, which has been previously reported by He et al. (2006). Moreover, similar results were obtained for the morphological changes of modified clay with different surfactants, such as tetramethylammonium chloride (TMA−Cl), hexadecyl trimethylammonium chloride (HDTMA-Cl) and benzyl triethylammonium bromide (BTEA-Br) (Lazo et al., 2008).

Moreover, Fig. 5a to 5f are SEM micrographs of an alginate bead (PAlg), and CPN beads identified as NCB1 and NCB3. It is noteworthy, that CPN (NCB1) referred to materials synthesized with B1-500 organo-modified clay mineral, and NCB3 referred to CPN synthesized with B3 synthetic clay mineral. PAlg beads have a very compact surface (Fig. 5a and d) with some folds due to the shrinkage of the material during the drying process, which is in concordance with a previous reported work (Kleinübing et al., 2013). On the other side, CPN (NCB1 and NCB3), Fig. 5e and f respectively, had a granular surface, randomly distributed into the material, which were very similar to the clay morphology (Fig. 5b). In the case of the CPN, clay mineral aggregates were homogeneously distributed on the surface of the material; meanwhile, in the PAlg bead (Fig. 6d), those aggregates were not present.

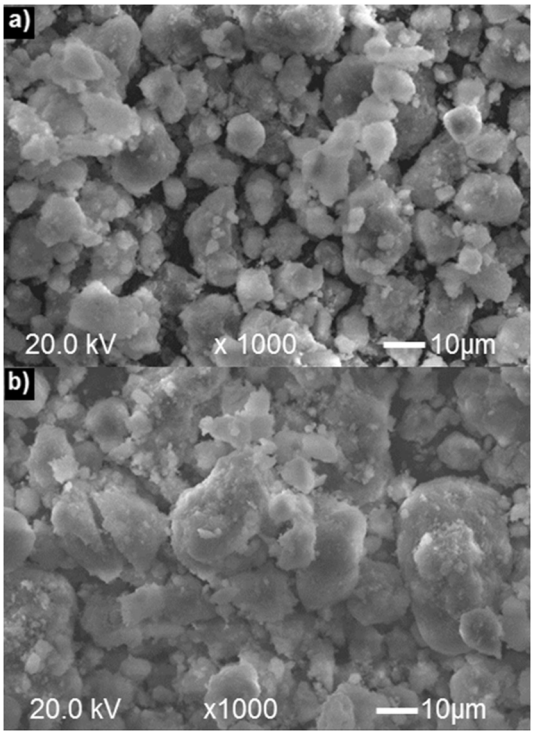

Fig. 4. SEM micrographs of a) raw clay mineral (B1) and b) HDTMA organo-modified clay mineral (B1-500).

3.2.2. FTIR analysis

FTIR spectra of cationic surfactant HDTMA and raw B1 and organo-modified B1-500 clay minerals were recorded and are illustrated in Fig. 6. Characteristic bands due to the stretching of the Si—O—Si and Al-OH bonds at 1000 cm^{-1} and 806 cm^{-1} were determined for the organo-modified clay mineral (B1-500); particularly, the bands due to the stretching (2935 cm^{-1} and 2838 cm^{-1}) and flexing (1452 cm^{-1}) of the methyl and methylene groups of the HDTMA aliphatic chain and the stretching band of the N—C bond (1490 cm^{-1}) indicates the successful modification of the Mt. with the cationic surfactant (Li et al., 2008; Zhang et al., 2012). Moreover, FTIR spectra of PAlg, NCB1, and modified clay mineral B1-500 were performed. In the case of NCB1, the stretching bands of the C═O carbonyl group (1595 cm^{-1}) and the stretching bands of the COO^- bond (1417 cm^{-1}) of the alginate were found; meanwhile, the stretching bands of the Si—O—Si (1030 cm^{-1}) and Al—OH (771 cm^{-1}) bonds corresponding to the clay, as well as the stretching bands of the methyl and methylene groups (2933 and 2842 cm^{-1}), confirmed the organo-modified clay mineral structure of the B1-500 incorporated into the alginate matrix structure (Van Hoogmoed et al., 2003; Deepa et al., 2016). Finally, FTIR of NCB3 confirmed the bands due to the stretching of the C═O group (1589 cm^{-1}) and the stretching bands of the COO^- group (1413 cm^{-1}) of the alginate, as well as the vibration bands of Si-OH and Al-OH bonds (1100 to 890 cm^{-1} and 790 cm^{-1}, respectively), and the stretching and flexion bands (2919, 2848 and 1465 cm^{-1}, respectively) of the methyl and methylene groups of the dimethyl dialkyl (C_{14}-C_{18}) amine surfactant, which were an indication of the incorporation of B3 clay mineral into the alginate structure.

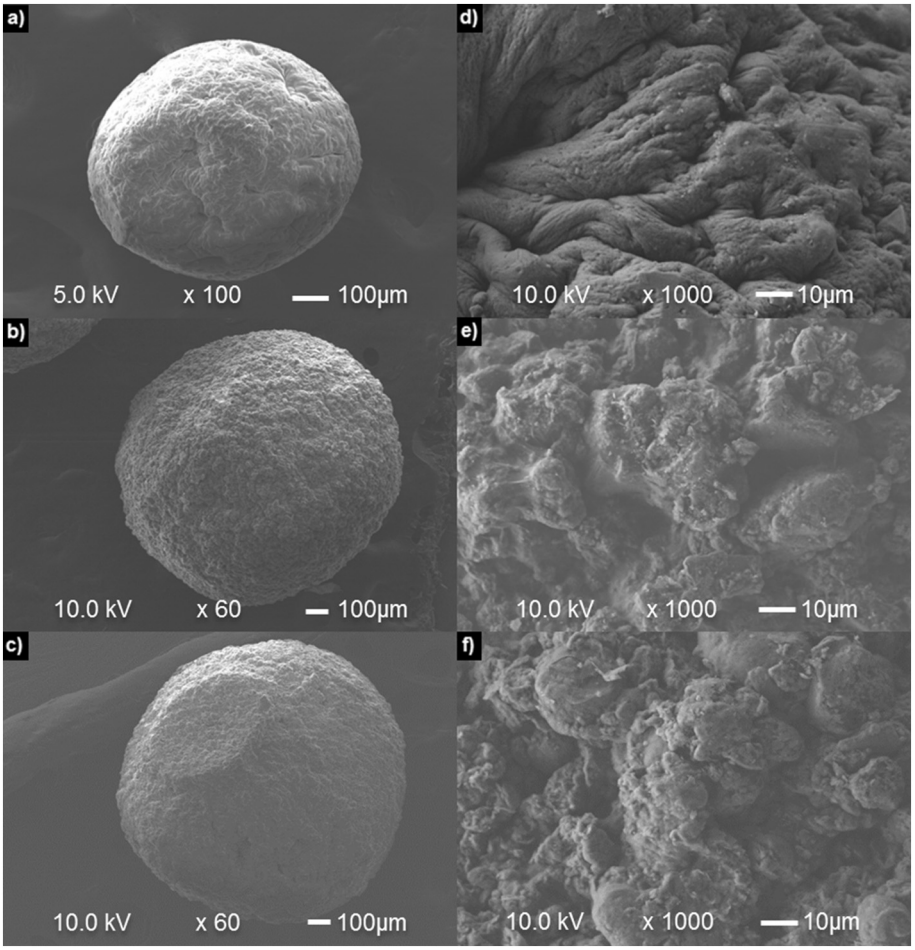

Fig. 5. SEM micrographs of a PAlg bead at a) 100× and d) 1000×, NCB1 bead (B1–500 clay mineral) at b) 100× and e) 1000×, and NCB3 bead (B3 clay mineral) at c) 100× and f) 1000×.

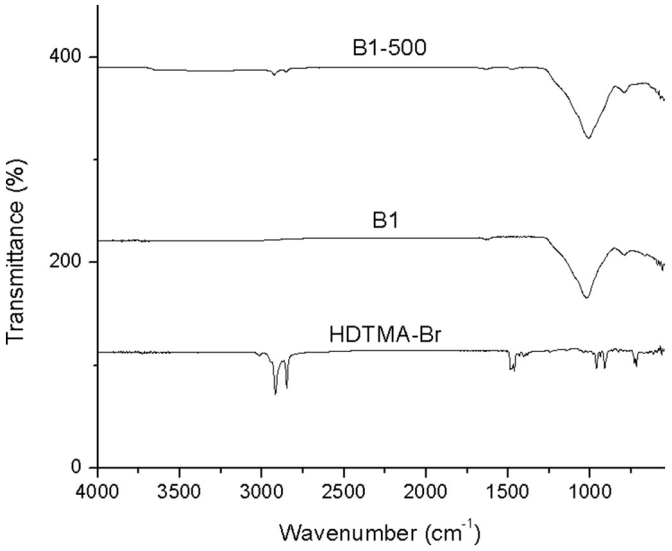

Fig. 6. FTIR spectra of raw clay (B1), organo-modified clay (B1-500) and cationic surfactant HDTMA.

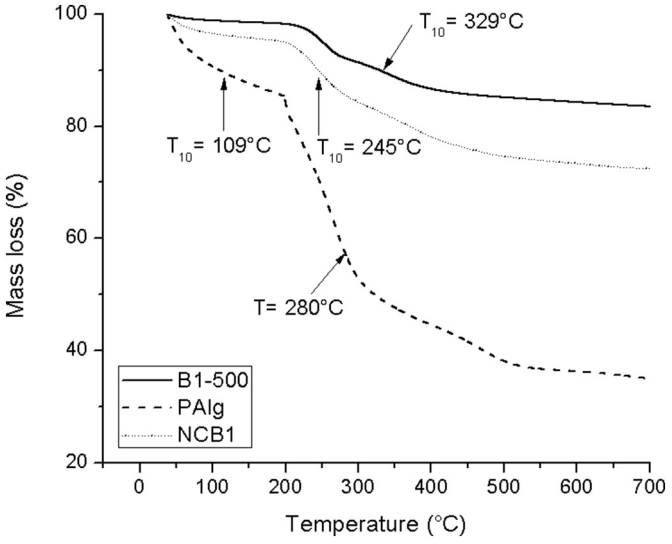

Fig. 7. TGA analysis of an alginate bead (PAlg), HDTMA organomodified clay (B1-500) and its CPN (NCB1).

3.2.3. Thermal properties of clays and the obtained CPN

Thermal properties of the clays and the obtained CPN were determined by TGA and DSC; in Fig. 7, the B1 Mt. presents a T_{10} (10% weight loss temperature) value of 465 °C, and a loss weight of 1% at 100 °C, and the organo-modified clay, B1-500, a T_{10} value of 329 °C and a mass loss of 7% at 100 °C. These results were an indication of the successful modification of the B1 Mt. with the organic surfactant HDTMA. In the case of the PAlg beads, the T_{10} value of 109 °C, corresponds to a drastic degradation between 250 and 350 °C. In the case of the NCB1, a T_{10} value of 245 °C was found with a moderate degradation temperature between 300 and 400 °C. Finally, NCB3 had a T_{10} value of 300 °C with a degradation temperature between 325 and 450 °C. These set of results indicated the successful incorporation of the organo-modified clay mineral into the CPN structures, since T_{10} temperature and materials degradation process changed with the stability of clays in the alginate structure.

In addition, the melting and glass transition temperatures were obtained by DSC (Fig. 8). The PAlg bead had a melting point around 100 °C, and for the HDTMA organo-modified clay, B1-500, only a glass transition temperature, Tg, of 50 °C was determined; however, when this organo-modified clay was incorporated into the PAlg bead, the melting point of the synthesized NCB1 had a degradation peak, less pronounced, and around 55 °C. This modification was an indication of the successful incorporation of the clay mineral into the PAlg matrix structure.

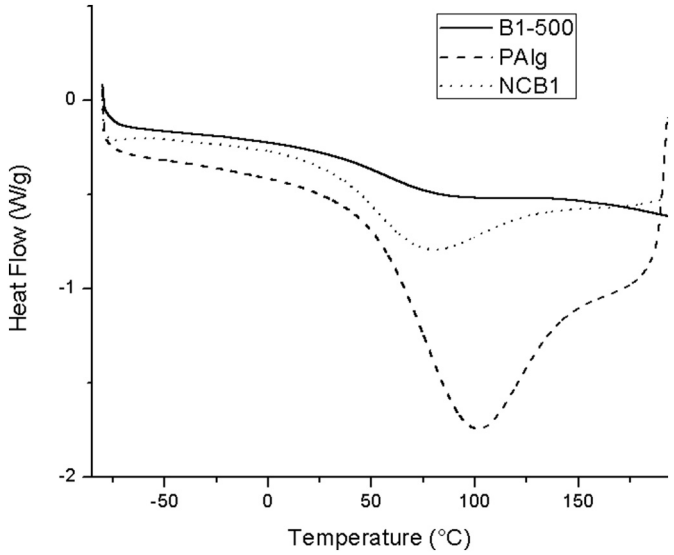

Fig. 8. DSC analysis of an alginate bead (PAlg), HDTMA organo-modified clay mineral (B1-500) and its CPN (NCB1).

3.2.4. Adsorption experiments

Different probes were performed to determine the adsorption capacity of the B1 and B1–500 clay minerals, as well as that of the PAlg, and NCB1, which are with and without the incorporation of the B1-500 clay mineral. The first contact test with the clay minerals was performed after 24 h. A comparison between B1 and B1-500 clays and B2 and B2-500 clays was done. The colloidal properties of the B2 and B2-500 clay minerals did not allow them to separate from the liquid phase, which represented interference for the subsequent quantification of phenol or 4CF. For this reason, the studied CPN were synthesized with both B1-500 and B3 clays, in order to compare the behavior of the clay mineral obtained from a natural source (B1-500) and a synthetic clay mineral (B3).

Adsorption capacities of phenol and 4CF with B1-500 Mt and CPN are illustrated in Figs. 9 and 10, respectively.

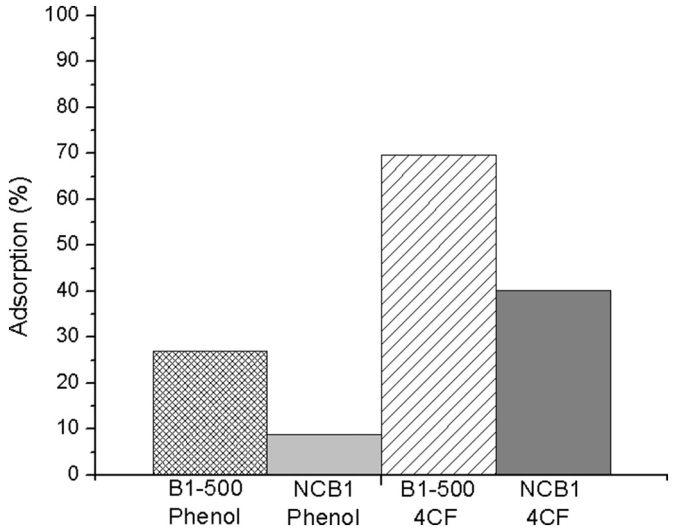

Fig. 9. Adsorption kinetics of phenol and 4CF with organo-modified clay, B1–500, and its CPN, NCB1.

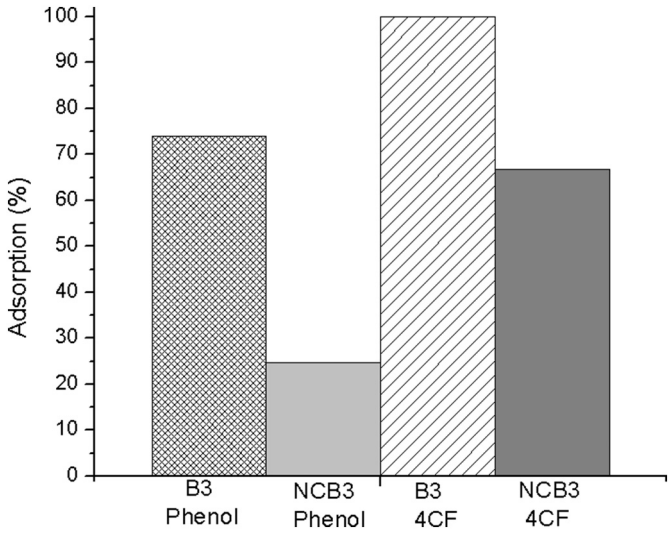

Fig. 10. Adsorption kinetics of phenol and 4CF with CPN (NCB3).

Fig. 9 illustrates the removal percentages of the phenolic compounds with the organo-modified clay mineral (B1-500) and its CPN (NCB1). From this graph, a higher preference of 4CF removal can be observed (up to 70% with clay and 40% with the CPN) compared to the removal of phenol (27% with clay and 9% with the CPN), which can be attributed to the difference in solubility of the molecules, which was higher for 4CF (27.1 $g{\cdot}L^{-1}$ at 25 °C) than for phenol (77.5 $g{\cdot}L^{-1}$ at 25 °C).

Fig. 10 depicts the adsorption process of the phenolic compounds with the B3 clay and its CPN (NCB3). In the case of the B3 clay-4CF system, a maximum removal capacity of qe = 0.496 $mg{\cdot}g^{-1}$ was reached, with an equilibrium time of 15 min; and for the B3-phenol system the qe value was found at qe = 0.377 $mg{\cdot}g^{-1}$ with an equilibrium time of 9 h. On the other side, NCB3 systems had a qe = 0.334 $mg{\cdot}g^{-1}$ for 4CF and qe = 0.118 $mg{\cdot}g^{-1}$ for phenol, respectively. In both cases, this removal process started after 3 h.

Similarly, Fig. 10 demonstrated an analogous tendency to remove 4CF, compared with phenol, with both materials: the synthetic organoclay mineral (B3) and its CPN (NCB3). For these materials, greater percentages of 4CF removal were obtained (74 and 100% with B3 clay and 25 and 67% with the NCB3) than those found with materials B1-500 and NCB1. This could be associated to the solubility of phenolic compounds in water, and also, because of the molecular structure of the surfactant which has two long alkyl chains in the B3 synthetic clay mineral, compared to the single chain of the HDTMA in the B1-500 organo-modified clay.

4. Conclusions

The modification of two raw clays with the cationic surfactant HDTMA and their incorporation into a PAlg bead were successfully achieved. FTIR spectra of HDTMA organo-modified clay, B1-500, confirmed the HDTMA presence. Moreover, XRD analysis demonstrated that HDTMA modification occurred more probably in the clay mineral surface. Furthermore, the organo-modified clay mineral was successfully incorporated to synthesized CPN. SEM micrographs illustrated a change in the morphology of PAlg beads. Further analysis of this incorporation was confirmed through TGA and DSC thermal analyses. Also, from these characterization techniques, it was corroborated that the degradation temperatures changed, to a lesser value, for the CPN, compared with PAlg beads. Finally, adsorption experiments demonstrated that the removal capacity by CPN was higher for 4CF than for phenol, which is in agreement with some previous studies.

Acknowledgements

We thank Omar Novelo and Josué Romero for their assistance and kind discussions of SEM micrographs; Adriana Tejeda and Eriseth Reyes for their assistance with XRD determination, and thermal analysis (TGA and DSC), respectively. K. A. Hernández-Hernández is grateful to CONACyT for scholarship. We also thank CONACyT (Project Cátedras CONACyT-3056) and TecNM (Project 5887.16-P) for financial support.

References

Anadão, P., 2012. Polymer/clay nanocomposites: concepts, researches, applications and trends for the future. In: Ebrahimi, F. (Ed.), Nanotechnology and Nanomaterials "Nanocomposites - New Trends and Developments" INTECH, pp. 1–16.

Barreca, S., Orecchio, S., Pace, A., 2014. The effect of montmorillonite clay in alginate gel beads for polychlorinated biphenyl adsorption: isothermal and kinetic studies. Appl. Clay Sci. 99, 220–228.

Bergaya, F., Lagaly, G., 2013. General introduction: clays, clay minerals, and clay science. In: Bergaya, F., Lagaly, G. (Eds.), Handbook of Clay Science. Developments of clay science Vol. 5. Elsevier, Amsterdam, pp. 1–19 (Chapter 1).

Bergaya, F., Jaber, M., Lambert, J.F., 2011. Clays and clay minerals. In: Galimberti, M. (Ed.), Rubber-Clay Nanocomposites. Science, Technology, and Applications. Wiley Publications, New York, pp. 3–44 (Chapter 1).

Bergaya, F., Detellier, C., Lambert, J.-F., Lagaly, G., 2013. Introduction to clay-polymer nanocomposites (CPN). In: Bergaya, F., Lagaly, G. (Eds.), Handbook of Clay Science. Developments of clay science Vol. 5. Elsevier, Amsterdam, pp. 655–677 (Chapter 13).

Biswas, M., Sinha Ray, S., 2001. Recent progress in synthesis and evaluation of polymer-montmorillonite nanocomposites. In: New Polymerization Techniques and Synthetic Methodologies. Advances in Polymer Science Vol. 155. Springer, Berlin, Heidelberg, pp. 167–221 (Chapter 3).

Cavallaro, G., Gianguzza, A., Lazzara, G., Milioto, S., Piazzese, D., 2013. Alginate gel beads filled with halloysite nanotubes. Appl. Clay Sci. 72, 132–137.

Deepa, B., Abraham, E., Pothan, L.A., Cordeiro, N., Faria, M., Thomas, S., 2016. Biodegradable nanocomposite films based on sodium alginate and cellulose nanofibrils. Materials 9 (50), 1–11.

Díaz-Nava, M.C., Olguín, M.T., Solache-Ríos, M., 2012. Adsorption of phenol onto surfactants modified bentonite. J. Incl. Phenom. Macro. Chem. 74, 67–75.

Feng, J., Ding, H., Yang, G., Wang, R., Li, S., Liao, J., Li, Z., Chen, D., 2017. Preparation of black-pearl reduced graphene oxide–sodium alginate hydrogel microspheres for adsorbing organic pollutants. J. Colloid. Interf. Sci. 508, 387–395.

Gacitua, E.W., Ballerini, A.A., Zhang, J., 2005. Polymer nanocomposites: synthetic and natural fillers a review. Maderas-Cienc. Tecnol. 7 (3), 159–178.

He, H., Frost, R.L., Bostrom, T., Yuan, P., Duong, L., Yang, D., Xi, Y., Kloprogge, J.T., 2006. Changes in the morphology of organoclays with $HDTMA^+$ surfactant loading. Appl. Clay Sci. 31, 262–271.

Kleinübing, S.J., Gaia, F., Bertagnolli, C., Carlos da Silva, M.G., 2013. Extraction of alginate biopolymer present in marine alga sargassum filipendula and bioadsorption of metallic ions. Mater. Res. 16 (2), 481–488.

Lazo, J.C., Navarro, A.E., Sun-Kou, M.R., Llanos, B.P., 2008. Síntesis y caracterización de arcillas organofílicas y su aplicación como adsorbentes del fenol. Rev. Soc. Quím. Perú 74 (1), 3–19.

Li, Z., Jiang, W.T., Hong, H., 2008. An FTIR investigation of hexadecyl trimethylammonium intercalation into rectorite. Spectrochim. Acta A 71, 1525–1534.

Munagapati, V.S., Kim, D.S., 2017. Equilibrium isotherms, kinetics, and thermodynamics studies for congo red adsorption using calcium alginate beads impregnated with nano-goethite. Ecotox. Environ. Safe. 141, 226–234.

Pandey, N., Shukla, S.K., Singh, N.B., 2017. Water purification by polymer nanocomposites: an overview. Nano. http://dx.doi.org/10.1080/20550324.2017.1329983.

Pavlidou, S., Papaspyrides, C.D., 2008. A review on polymer layered silicate nanocomposites. Prog. Polym. Sci. 33, 1119–1198.

Silva, R.M.P., Manso, J.P.H., Rodrigues, J.R.C., Lagoa, R.J.L., 2008. A comparative study of alginate beads and an ion-exchange resin for the removal of heavy metals from a metal plating effluent. J. Environ. Sci. Health Part A 43 (11), 1311–1317.

Sinha Ray, P., 2013. Clay-containing polymer nanocomposites, from fundamentals to real applications. Elsevier Publishing, UK, pp. 1–37.

Sinha Ray, S., Okamoto, M., 2003. Polymer/layered silicate nanocomposites: a review from preparation to processing. Prog. Polym. Sci. 28, 1539–1641.

Van Hoogmoed, C.G., Busscher, H.J., De Vos, P., 2003. Fourier transform infrared spectroscopy studies of alginate–PLL capsules with varying compositions. J. Biomed. Mater. Res. 67A (1), 172–178.

Zhang, Y., Zhao, Y., Zhu, Y., Wu, H., Wang, H., Lu, W., 2012. Adsorption of mixed cationic-nonionic surfactant and its effect on bentonite structure. J. Environ. Sci. 24 (8), 1525–1532.

Zhiyu, Z., Kecen, X., Yu, C., 2017. Preparation and application of the composite from alginate. In: Thakur, V.K., Thakur, M.K., Kessler, M.R. (Eds.), Handbook of Composites from Renewable Materials, Design and Manufacturing. Vol. 2. Wiley, New Jersey, USA, pp. 341–376 (Chapter 14).